

RESEARCH

Open Access



Integrated metabolomic and transcriptomic analyses of regulatory mechanisms associated with uniconazole-induced dwarfism in banana

Liuyan Qin^{1,2}, Chaosheng Li^{1,2*}, Chenglin Guo³, Liping Wei^{1,2}, Dandan Tian^{1,2}, Baoshen Li^{1,2}, Di Wei^{1,2}, Wei Zhou^{1,2}, Shengfeng Long^{1,2}, Zhangfei He^{1,2}, Sumei Huang^{1,2} and Shaolong Wei^{1,2*}

Abstract

Background: Uniconazole is an effective plant growth regulator that can be used in banana cultivation to promote dwarfing and enhance lodging resistance. However, the mechanisms underlying banana dwarfing induced by uniconazole are unknown. In uniconazole-treated bananas, gibberellin (GA) was downregulated compared to the control groups. An integrative analysis of transcriptomes and metabolomes was performed on dwarf bananas induced by uniconazole and control groups. The key pathways involved in uniconazole-induced dwarfism in banana were determined according to the overlap of KEGG annotation of differentially expressed genes and (DEGs) differential abundant metabolites (DAMs).

Results: Compared with the control groups, the levels of some flavonoids, tannins, and alkaloids increased, and those of most lipids, amino acids and derivatives, organic acids, nucleotides and derivatives, and terpenoids decreased in uniconazole-treated bananas. Metabolome analysis revealed the significant changes of flavonoids in uniconazole-treated bananas compared to control samples at both 15 days and 25 days post treatment. Transcriptome analysis shows that the DEGs between the treatment and control groups were related to a series of metabolic pathways, including lignin biosynthesis, phenylpropanoid metabolism, and peroxidase activity. Comprehensive analysis of the key pathways of co-enrichment of DEGs and DAMs from 15 d to 25 d after uniconazole treatment shows that flavonoid biosynthesis was upregulated.

Conclusions: In addition to the decrease in GA, the increase in tannin procyanidin B1 may contribute to dwarfing of banana plants by inhibiting the activity of GA. The increased of flavonoid biosynthesis and the change of lignin biosynthesis may lead to dwarfing phenotype of banana plants. This study expands our understanding of the mechanisms underlying uniconazole-induced banana dwarfing.

Keywords: Banana dwarfing, Uniconazole, Metabolome, Transcriptome, Flavonoid synthesis

Background

Dwarfing, an important agronomic trait, has been a research hotspot for breeders. Varieties with dwarfing characteristics not only have unique advantages in production management but also have great potential in terms of high yield. In the production of bananas (*Musa* spp.), the stems of tall bananas are easily damaged by typhoons and require additional support costs. Production efficiency can be optimized by controlling grass

*Correspondence: lcs@gxaas.net; weishaolong@gxaas.net

¹ Biotechnology Research Institute, Guangxi Academy of Agricultural Sciences, Nanning 530007, China

Full list of author information is available at the end of the article



© The Author(s) 2022. **Open Access** This article is licensed under a Creative Commons Attribution 4.0 International License, which permits use, sharing, adaptation, distribution and reproduction in any medium or format, as long as you give appropriate credit to the original author(s) and the source, provide a link to the Creative Commons licence, and indicate if changes were made. The images or other third party material in this article are included in the article's Creative Commons licence, unless indicated otherwise in a credit line to the material. If material is not included in the article's Creative Commons licence and your intended use is not permitted by statutory regulation or exceeds the permitted use, you will need to obtain permission directly from the copyright holder. To view a copy of this licence, visit <http://creativecommons.org/licenses/by/4.0/>. The Creative Commons Public Domain Dedication waiver (<http://creativecommons.org/publicdomain/zero/1.0/>) applies to the data made available in this article, unless otherwise stated in a credit line to the data.

growth in bananas. Semi-dwarf banana varieties are resistant to wind and rain damage [1]. In addition, an increase in yield associated with short stems is associated with an increase in the harvest index [2]. The crouching physique of dwarf banana varieties can resist the harm of typhoons to a certain extent and has the advantages of convenient cultivation, field management, labor saving, and dense planting [3]. The dwarf variant is also helpful for mining and researching dwarf-related genes. The identification and utilization of dwarf-related banana genes are very important for breeding dwarf banana varieties.

Plant height traits are not only controlled by internal genes, but are also affected by various hormones and external environmental factors [4]. Studies have found that most dwarf mutations are caused by changes in the growth and development of plant stems owing to mutations in hormone synthesis pathways or response regulation [5]. Many dwarf mutants are related to plant gibberellins (GAs) and brassinosteroids, whereas several mutations are related to auxins [6, 7]. By analyzing plant hormone synthesis and signaling mutants and treating plants with exogenous hormone spray, it was found that GAs and brassinosteroids regulate the expansion of plant cells and organs along the longitudinal axis, greatly affecting plant height and organ size [8]. They are the main hormones that cause plant dwarfing. Uniconazole, a highly effective plant growth inhibitor, hinders the oxidative demethylation of kaurene to kaurenoic acid, making it difficult to synthesize kaurenoic acid and thereby cutting off the biosynthesis of GAs [9]. At the same time, it is an effective dwarf plant inducer [10]. At present, the application of uniconazole in fruits is mainly used to control vegetative growth, promote plant rooting and flower formation, promote seed filling, improve fruit quality, increase yield, and enhance stress resistance [11, 12]. Previous studies on the dwarfing mechanisms of model plants such as *Arabidopsis thaliana* and rice have been conducted, and it is believed that plant dwarfing is mainly regulated by plant hormones [4]. However, few studies have been conducted on the causes and mechanisms underlying banana dwarfing.

GAs play a fundamental role in plant growth and development and are involved in regulating a variety of developmental processes. The reduction in reactive GAs content results in plants exhibiting a dwarf phenotype. The GA biosynthetic pathway is well understood in model plants and related variants have been isolated [5, 13, 14]. GAs are biosynthesized from geranyl diphosphate, which is a common C₂₀ precursor of diterpenoids. GA20ox, GA3ox, and GA2ox are enzymes that catalyze late reactions in the GA biosynthetic pathway and belong to the 2OG-Fe (II) oxidase superfamily. In many plant

species, enzymes are independently encoded by different gene families [15] and thus have functional redundancy and tissue specificity [16]. The loss-of-function of these GA oxidase genes (except GA2ox) in plants produces a dwarf phenotype that can be restored by the application of exogenous GA [16–19]. For example, the well-known Green Revolution gene *sd-1* is generated by the loss-of-function of *OsGA20ox2* in rice [20]. Conversely, GA2ox reduces the levels of reactive GAs in plants, and overexpression of GA2ox leads to dwarf plants [21, 22]. Chen et al. revealed that *MaGA20ox4*, *MaGA20ox5*, *MaGA20ox7*, *MaGA2ox7*, *MaGA2ox12*, and *MaGA2ox14* are the main genes regulating the GA content difference between 8818 and its dwarf mutant, 8818–1, and each gene may perform different functions in different tissues or during different developmental stages [1].

Banana genome sequencing was completed in 2012 [23], but related information on dwarfism metabolism in bananas is limited. The genes, pathways, and metabolites associated with dwarfism induced by uniconazole in bananas have not been explored. In this study, an integrative analysis of transcriptomes and metabolomes was performed on uniconazole-induced bananas to investigate the regulatory mechanisms of dwarfism during banana development. The results of this study provide both candidate genes and novel approaches that can be used to produce improved banana traits.

Results

Characterization of uniconazole-induced dwarfism in banana

To confirm the effect of uniconazole on dwarfism in bananas, we designed a concentration gradient (0.1 g, 0.3 g, and 0.5 g) and compared the induced traits (Fig. 1). The plants in the control group exhibited a height of approximately 220 cm with normal banana stalks (Fig. 1A), and plants dwarfed to approximately 170 cm when treated with 0.1 g uniconazole (Fig. 1B). Treatment with 0.3 g uniconazole further dwarfed the plants to approximately 140 cm with short comb spacing (Fig. 1C), whereas an overdose of uniconazole (0.5 g) induced malformation of buds and a height of 135 cm (Fig. 1D).

Physiological and biochemical changes in uniconazole-induced dwarf banana

GA content was significantly downregulated in uniconazole-treated bananas. The lowest GA content was observed for both groups treated with 0.3 g and 0.5 g uniconazole (Fig. 2A). A considerable number of physiological and biochemical indices, including potassium, calcium, magnesium, phosphorus, soluble protein, and SOD activity, increased as the concentration gradient

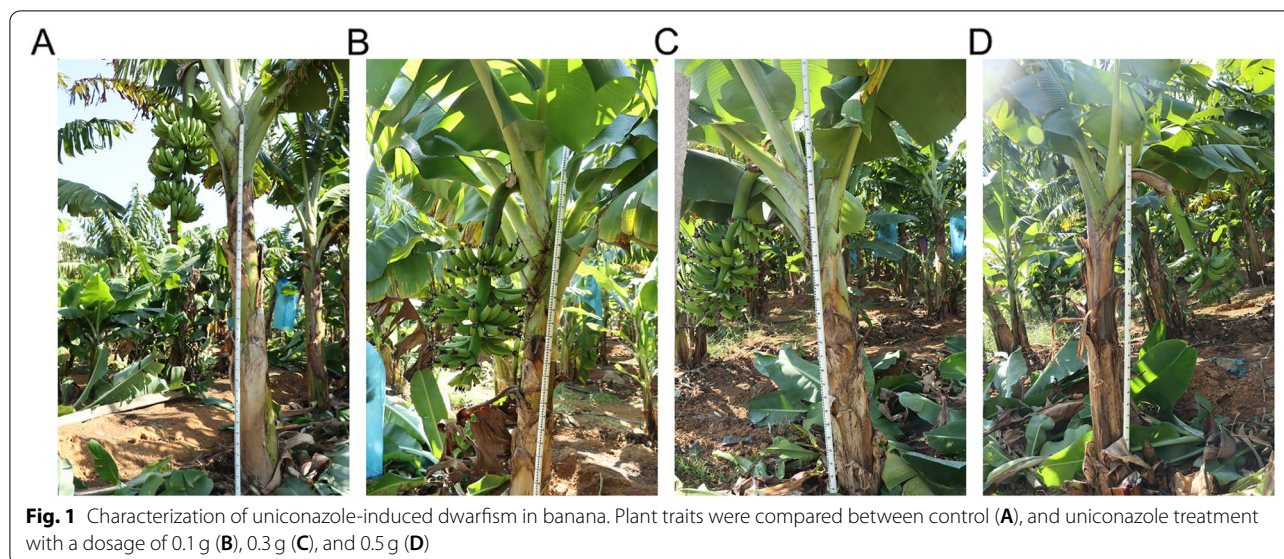


Fig. 1 Characterization of uniconazole-induced dwarfism in banana. Plant traits were compared between control (A), and uniconazole treatment with a dosage of 0.1 g (B), 0.3 g (C), and 0.5 g (D)

of uniconazole increased. In contrast, the levels of these indices in the control and paclobutrazol-treated groups were the lowest and highest, respectively (Fig. 2B–2I). In addition, the enzyme activities of CAT, PAL, and PPO showed a similar trend (Fig. 2J–2L). Consequently, the dosage of 0.3 g uniconazole was chosen for further metabolomic and transcriptomic experiments based on to the best dwarfism traits induced in banana and the minimum effect on physiological and biochemical indices.

Metabolomic changes associated with uniconazole-induced dwarfism

A total of 1082 metabolites were identified based on the metabolomics data (Table S1), which showed a high correlation ($r > 0.9$) between replicates within groups (Fig. S1A). PCA showed clustering of samples into distinct groups and stages, and the treatment group was closer to the control group at 25 d than at 15 d (Fig. S1B).

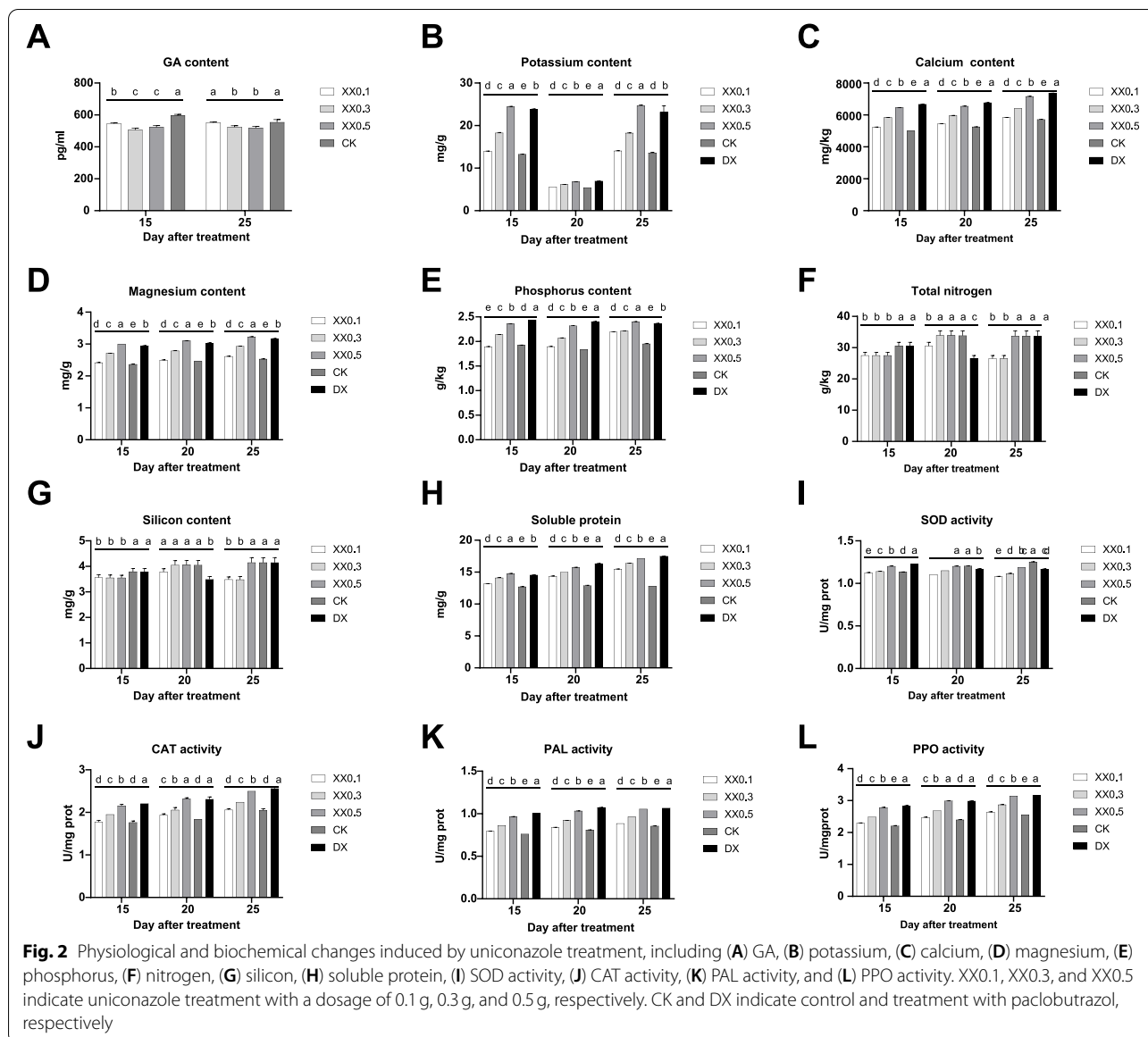
A considerable number of differential abundant metabolites (DAMs) were identified between the treatment and control groups at 15 d (Fig. 3A). Among them, the levels of most differential flavonoids, tannins, and alkaloids increased after uniconazole induction, whereas those of most lipids, amino acids and derivatives, organic acids, nucleotides and derivatives, and terpenoids decreased (Fig. 3A). These DAMs were significantly enriched in flavone and flavonol biosynthesis, betalain biosynthesis, flavonoid biosynthesis, isoquinoline alkaloid biosynthesis, thiamine metabolism, and phenylpropanoid biosynthesis pathways (Fig. 3B). Meanwhile, the levels of differential flavonoids and tannins also increased when treated with uniconazole at 25 d (Fig. 4A), and the differential

metabolites participated in flavonoid biosynthesis, phenylpropanoid biosynthesis, and plant hormone signal transduction pathways (Fig. 4B). The common DAM between 15 d and 25 d showed a similar trend, including three downregulated ($3'$ -adenylic acid, gentiopicric acid, and lysoPC 18:4) and 19 upregulated metabolites, including mainly flavonoids (pinobanksin, epicatechin-epiafzelechin, apigenin-6-C-($2'$ -glucuronyl) xyloside, kaempferol-3,7-O-dirhamnoside (kaempferitrin), vitexin- $2''$ -O-rhamnoside, pelargonidin-3-O-rutinoside, and catechin-catechin-catechin), and tannins (such as procyanidin, cinnamtannin, and arecatannin) (Table S2).

Global transcriptomic changes in response to uniconazole-induced dwarfism

After the removal of low-quality reads, a minimum of 40 million clean reads were obtained for each sample and mapped to the reference genome at a high mapping rate ($> 91\%$) (Table S3). A high correlation ($r \geq 0.87$) was observed between replicates within groups for transcriptomic data (Fig. S2A), and PCA analysis shows similar clusters with the metabolomics data (Figs. S1B and S2B).

Differentially expressed genes (DEGs) between the treatment and control groups at 15 d were identified (Fig. 5A), which are involved in photosynthesis and oxidative phosphorylation pathways (Fig. 5B) and associated with photosynthesis, response to cytokinin, xylem development, and phenylpropanoid biosynthetic process (Fig. 5C). DEG identified at 25 d (Fig. 6A) were enriched in protein processing in the endoplasmic reticulum, tyrosine metabolism, and isoquinoline alkaloid biosynthesis pathways (Fig. 6B) and associated with tyrosine metabolic process, fatty acid biosynthetic process,



oxylipin biosynthetic process, suberin biosynthetic process, lipid oxidation, phenylpropanoid metabolic process, and peroxidase activity (Fig. 6C). No common DEG were observed between 15 d and 25 d.

Key pathways involved in uniconazole-induced dwarfism in banana

The common enriched pathways for both DEG and DAM between 15 d and 25 d were further examined, which included four key pathways: metabolic pathways, phenylpropanoid biosynthesis, flavonoid biosynthesis, and biosynthesis of secondary metabolites (Fig. 7A). Of these, the phenylpropanoid biosynthesis pathway comprises flavonoid biosynthesis. We further examined

the differential factors in the phenylpropanoid biosynthesis pathway and found that the expression levels of shikimate O-hydroxycinnamoyltransferase (HCT) and peroxidase, and the abundance of pinobanksin, vitexin, and epigallocatechol increased in uniconazole-treated bananas compared with the control group (Fig. 7B). The quantitative real-time PCR (qRT-PCR) analysis also confirmed the overexpression of HCT and peroxidase genes in treatment group (Fig. S3).

Discussion

Bananas treated with uniconazole showed a significant dwarf phenotype, indicating that the dwarfing induction was successful. The physiological and biochemical

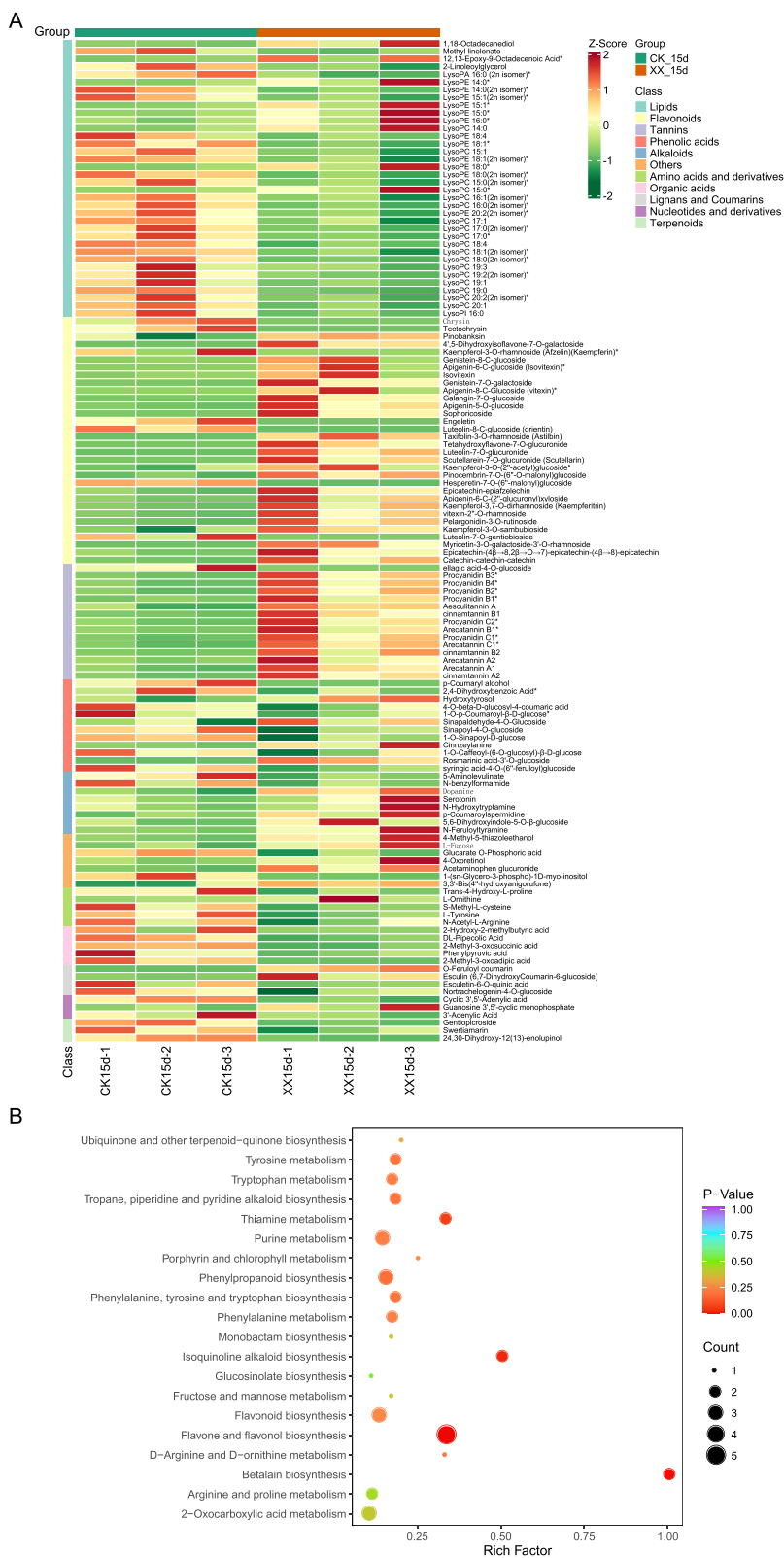


Fig. 3 Differential metabolites (DAM) between the treatment and control groups at 15 d. **A** Heatmap representing the level of DAM across groups. **B** KEGG pathway enrichment analysis of the DAM identified in (A). XX indicate uniconazole treatment, and CK indicate control

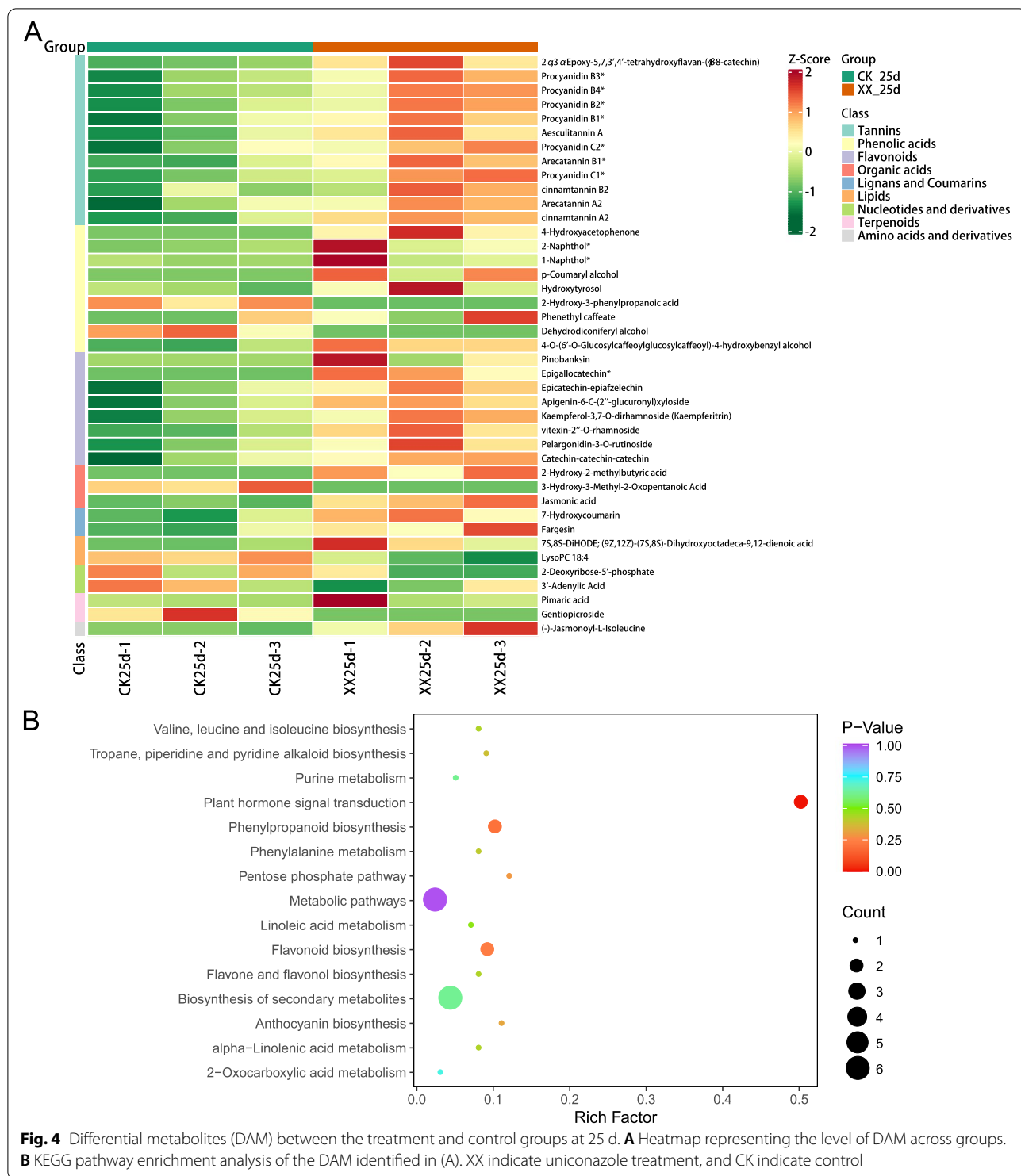
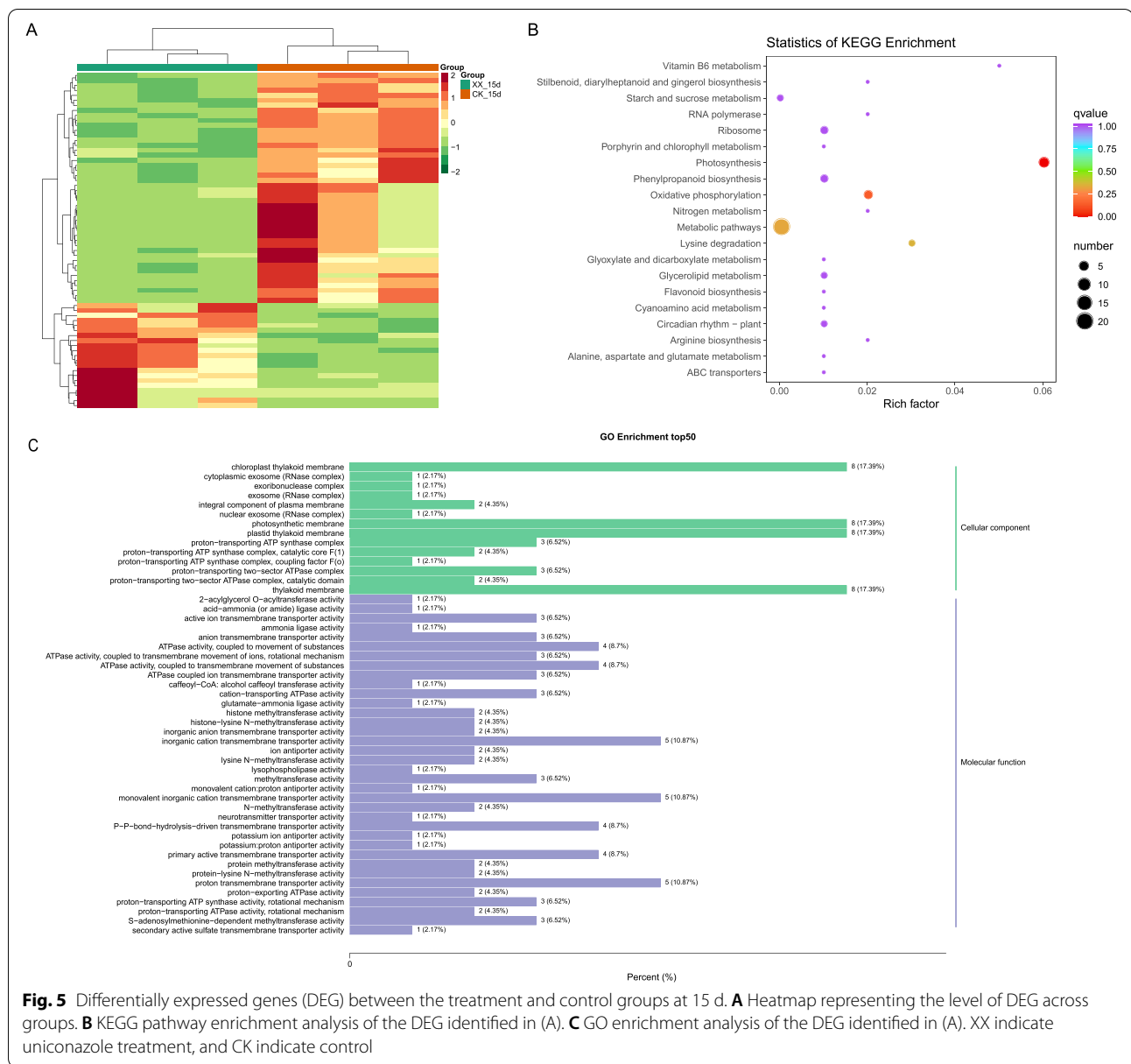


Fig. 4 Differential metabolites (DAM) between the treatment and control groups at 25 d. **A** Heatmap representing the level of DAM across groups. **B** KEGG pathway enrichment analysis of the DAM identified in (A). XX indicate uniconazole treatment, and CK indicate control

indexes of the treated group were also significantly different from those of the control group, and GA was significantly reduced in the treated group.

In previous studies, the biosynthesis of flavonoids and alkaloids has been reported to be activated in dwarfing

plants, and tannins are associated with plant dwarfing. It has previously been reported that the biosynthesis or accumulation of flavonoids changes significantly in a variety of dwarf plants compared with the higher group. The expression levels of some flavonoid biosynthesis



genes are significantly different in the dwarf Polish wheat mutant *Rht1* than in high Polish wheat. These changes increase flavonoid content [24]. *Rht1* gene encodes a GA signaling repressor that reduces the response to GA and limits the elongation of wheat stems [2, 25]. In *Seashore paspalum*, the dwarf phenotype of mutant *TS1* is considered to be closely related to the upregulation of flavonoid biosynthesis in the phenylpropanoid pathway [26]. Over-accumulation of flavonoids has been reported not only in dwarf herbs, but also in woody apple dwarfing rootstocks [27]. Isoquinoline alkaloid biosynthesis was reported to be activated in the dwarf wheat infected with *Tilletia controversa* Kühn [28]. In our results, a variety

of flavonoids were increased, and increased alkaloids were significantly enriched in isoquinoline alkaloids in the uniconazole-treated banana, similar to the changes previously reported in the dwarfing plants mentioned above. Various tannins have been reported to inhibit GA-induced plant growth [29, 30]. Although uniconazole was considered an inhibitor of GA biosynthesis in previous reports, we found no significant changes related to the GA biosynthesis pathway in bananas treated with uniconazole [9, 31]. The reported GA inhibitor tannin procyanidin B1 was increased in bananas treated with uniconazole, suggesting that reduced GA levels are not the only factor responsible for banana dwarfing, as the

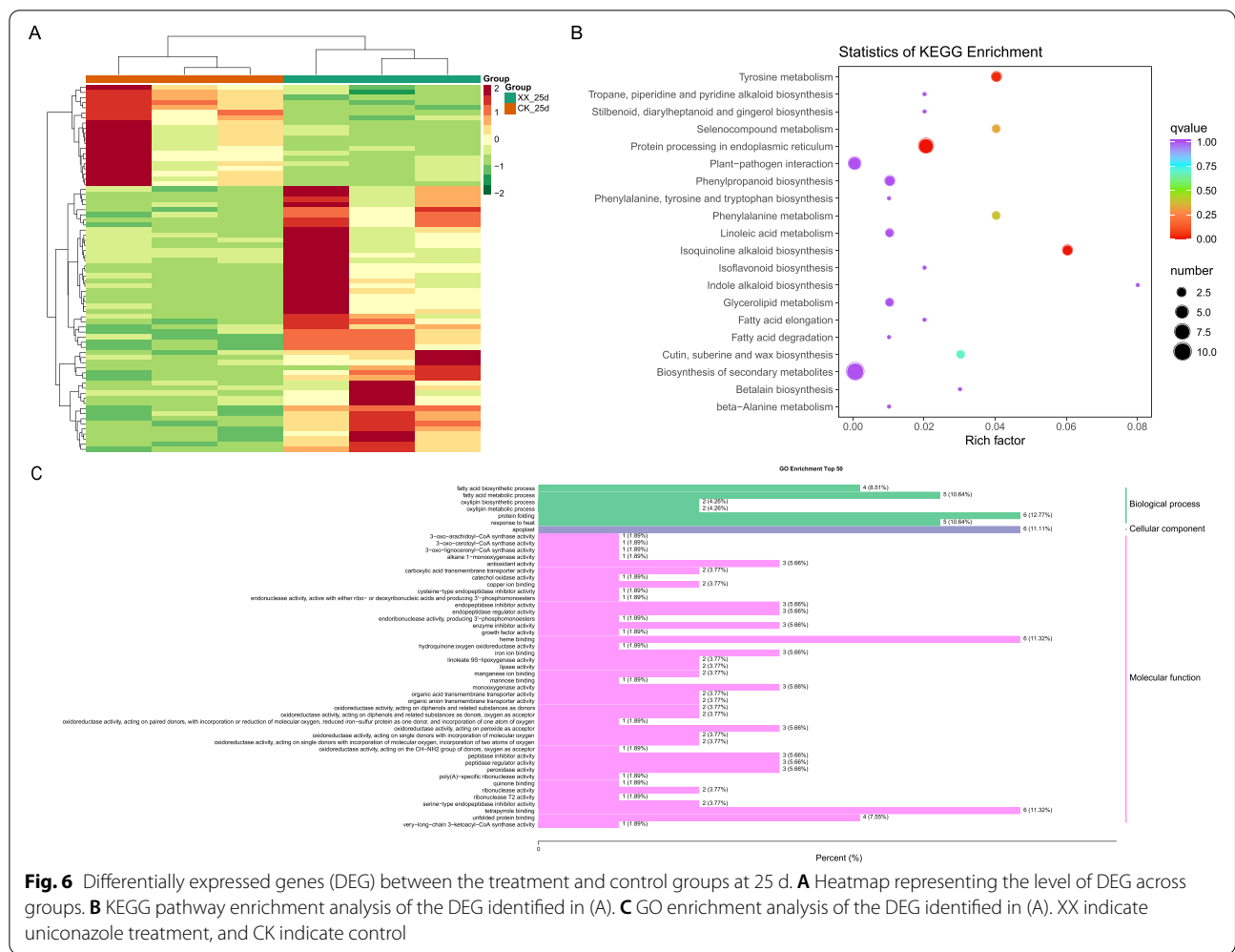
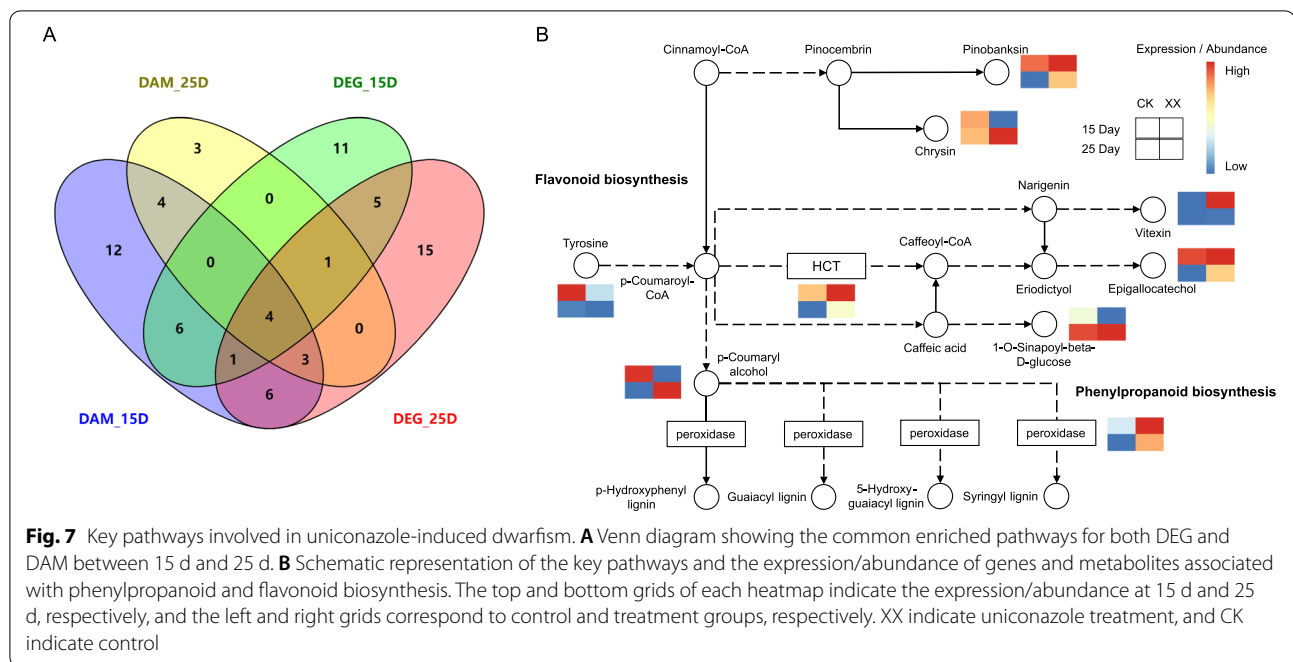


Fig. 6 Differentially expressed genes (DEG) between the treatment and control groups at 25 d. **A** Heatmap representing the level of DEG across groups. **B** KEGG pathway enrichment analysis of the DEG identified in (A). **C** GO enrichment analysis of the DEG identified in (A). XX indicate uniconazole treatment, and CK indicate control

over-accumulation of tannins may inhibit GA activity and cause banana dwarfing [30]. We propose that increased levels of flavonoids, isoquinoline alkaloids, and tannins play important roles in uniconazole-induced dwarfing.

The phenylpropanoid pathway is involved in several physiological processes. In addition to flavonoid biosynthesis, the lignin synthesis pathway is involved in the phenylpropanoid pathway [32–35]. Previous studies have reported that the knockout or knockdown of one or more genes of the phenylpropanoid pathway can lead to dwarfism by reducing the lignin content [36]. Lignin is a complex, aromatic polymer mainly presenting in secondarily thickened cell walls and provides rigidity, strength, and hydrophobicity [37–39]. In some dwarf plants with enhanced flavonoid biosynthesis, lignin biosynthesis is downregulated. Compared with high Polish wheat, the expression levels of some lignin are significantly different in the dwarf Polish wheat mutants *Rht1*, leading to lignin level reduction [24]. In *S. paspalum*, the dwarf phenotype of mutant *T51* is considered to be closely related not only

to the upregulation of flavonoid biosynthesis, but also to the downregulation of lignin biosynthesis [26]. In addition, delayed lignin accumulation was found in dwarfed transgenic rice expressing the α -L-arabinofuranosidase of *Coprinopsis cinerea* [40]. However, in some plants, lignin accumulation was also found to be detrimental to plant growth. Leaf, root and stem growth were significantly enhanced in transgenic aspen with the lignin biosynthetic pathway gene *Pt4CL1* downregulated [41]. In addition, banana plants overexpressed with VND1, VND2 or VND3 had increased lignin deposition. These transgenic banana plants showed stunted growth [42, 43]. Moreover, the reduction of lignin was observed in transgenic bananas overexpressing *MusaNAC68* and was considered to be linked with the increase in the height of transgenic bananas [44]. Although peroxidase increased in uniconazole-treated bananas at both 15 d and 25 d, p-coumaryl alcohol, the substrate of peroxidase, only increased at 25 d and decreased at 15 d. At 25 d, peroxidase expression was lower than that at 15 d. The inconsistency in the time



and degree of change of the substrate p-coumaroyl alcohol and peroxidase could not provide sufficient evidence for the change in lignin biosynthesis. In addition, some other genes or metabolites in the phenylpropanoid synthesis pathway that are not involved in lignin biosynthesis also increased significantly under uniconazole treatment. P-Coumaroyl-CoA can be converted to p-coumaroyl alcohol or to the flavonoid epigallocatechol. HCT is an enzyme involved in the conversion of p-coumaroyl-CoA to epigallocatechol [45]. Both HCT and epigallocatechol increased in uniconazole-treated bananas at 15 d and 25 d. These results suggest that the enhanced biosynthesis of flavonoids may reduce the metabolic flux of lignin. The important plant hormone auxin and several auxin responsive factors (ARFs) have also been reported to regulate lignin synthesis, and *MYB* gene has previously been reported to be involved in auxin response and endothe-cium lignification of anther walls [46]. The substantial elevation of *MYB* transcription factors such as *MYB4a-like* and *MYB4b-like* factors was observed in transgenic bananas overexpressing *MusaNAC68* [44]. However, no significant changes in the expression of *ARF* and *MYB* genes were identified in the uniconazole-treated bananas. The mechanism of dwarfism in uniconazole-treated bananas may be related to lignin biosynthesis during stem elongation, but the specific effect of lignin biosynthesis on banana growth need to be further studied.

In summary, in addition to a decrease in GA content, an increase in tannin procyanidin B1 content may contribute to banana dwarfing by inhibiting GA activity.

Flavonoids and lignin are metabolites of the phenylpropanoid pathway, and there is a competitive relationship between them. The increase in flavonoid biosynthesis promoted the increased flow of metabolites towards flavonoid synthesis, which indirectly led to a decrease in lignin biosynthesis. Based on the above results, we propose a uniconazole-induced dwarfing mechanism hypothesis: over-accumulation of tannin inhibits the role of GA in banana growth, and abnormal lignin synthesis affects cell wall function, ultimately limiting cell expansion and causing dwarfism in uniconazole-treated bananas.

Materials and methods

Plant materials and treatment

Experiments were performed at the Libang Scientific Base of Guangxi Academy of Agricultural Sciences, located in Futang town in Wu Ming district, Nanning city, Guangxi province, China. The banana cultivar 'Guijiao No.9' was used, and the seeds were planted in January, 2021. We got the permission to collect Banana seeds. And the study protocol was complied with relevant institutional, national, and international guidelines and legislation. Uniconazole wettable powder (5%, Sichuan Runer Technology, China) was applied to the plants when they grew to 16–18 leaves. The powder was diluted to obtain different concentration gradients, and then 200 mL solutions were drenched along the base of the pseudostem, resulting a gradient dosage of 0.1 g/plant, 0.3 g/plant, and 0.5 g/plant. Plants treated with water at the same

stage as described above were used as controls. Twenty plants were used for each uniconazole-treated and control group and used to measure the dwarfed phenotype. Leaves were collected at 15, 20, and 25 d after treatment for both the uniconazole-induced and control groups. A total of 100 g of leaf blade (without leaf vein) was clipped from the penultimate piece of leaf for each plant and immediately frozen in liquid nitrogen or stored in a refrigerator at -80°C . Three independent biological replicates were conducted for the subsequent measurement of physiological indices, cDNA library construction, and RNA sequencing for each uniconazole-treated and control group.

Measurement of physiological indices

GA production was estimated using a tetramethyl benzidine (TMB) detection system after incubation with an HRP-conjugated antibody. GA content was quantified by measuring the absorbance at 450 nm. Other physiological indices of the leaf samples were assessed using a spectrophotometric method. Polyphenol oxidase (PPO) activity was assayed using pyrocatechol as the substrate. Superoxide dismutase (SOD) activity was measured using the xanthine oxidase method based on the production of $\text{O}_2^{\cdot-}$. Catalase (CAT) activity was examined by measuring H_2O_2 decomposition. Phenylalanine ammonia-lyase (PAL) activity was measured from the conversion of l-phenylalanine to trans-cinnamic acid. Soluble protein was quantified based on the reduction of Cu^{2+} to Cu^{1+} in an alkaline environment. PPO, SOD, CAT, PAL, and soluble protein activities were determined by measuring the absorbance at 410, 450, 240, 290, and 562 nm, respectively, and expressed as units/mg protein.

Measurement of biochemical indices

The potassium, calcium, and magnesium contents were determined by atomic absorption spectroscopy (AAS, TAS-900 AFG, China). Total phosphorus content was measured using phosphorus molybdenum blue spectrophotometry at 660 nm, and total phosphorus was expressed as the concentrations of organic and inorganic phosphorus. Total nitrogen was determined by titration with ferrous ammonium sulfate using an azotometer. Si concentration was quantified using plasma atomic emission spectroscopy (ICP-AES).

Metabolite extraction and LC-MS/MS analysis

Leaf samples were freeze-dried and crushed using a mixer mill (MM 400, Retsch). Lyophilized powder (100 mg) was dissolved in 1.2 mL of 70% methanol solution and kept at 4°C overnight. After centrifugation at 12000 rpm for 10 min, the extracts were filtered (SCAA-104, 0.22 μm pore size; ANPEL, Shanghai, China). UPLC

separation was performed using a 1.8 μm , 2.1 mm * 100 mm Agilent SB-C18 column. Linear ion trap (LIT) and triple quadrupole (QQQ) scans were acquired on an Applied Biosystems 4500 Q TRAP LC-MS/MS system, including an ESI Turbo ion-spray interface.

Metabolites were extracted and identified using the Metware database (Metware Biotechnology, Wuhan, China). VIP values for the identified metabolites were determined by OPLS-DA analysis using the R package MetaboAnalystR. Significantly regulated metabolites between groups were determined by $\text{VIP} \geq 1$ and absolute $\log_2\text{FC}$ (fold-change) ≥ 1 and were then subjected to metabolite set enrichment analysis (MSEA).

RNA extraction and RNA-Seq analysis

Total RNA was extracted from leaf samples using the Qiagen RNeasy Plant Kit (Hilden, Germany), according to the manufacturer's protocol. mRNAs were enriched by poly(A) selection from the extracted total RNA, and rRNA-depleted samples were prepared using the Illumina TruSeq RNA Sample Prep Kit to obtain a strand-specific library. Purification and size selection of cDNA were performed using AMPure XP beads, resulting in a median fragment size of 300 bp. The cDNA libraries were then checked using Qubit2.0, Agilent 2100, and sequenced using the Illumina Novaseq platform.

Raw data were preprocessed using fastp (v0.19.3) with parameters “-n_base_limit 15 -qualified_quality_phred 20,” and clean reads were then aligned to the banana reference genome (NCBI accession No. GCF_000313855.2) with HISAT2 (v2.1.0). Gene expression levels were quantified using featureCounts (v1.6.1), and fragments per kilobase of transcript per million fragments mapped (FPKM) was calculated. Pearson's correlation coefficients between samples were computed, and principal component analysis (PCA) was performed based on gene expression levels. DESeq2 (v1.22.1) was used to perform differential gene expression analysis between groups. Genes with $|\log_2\text{foldchang}| \geq 1$ and $\text{FDR} < 0.05$ were identified as significantly DEG. Gene ontology (GO) and Kyoto Encyclopedia of Genes and Genomes (KEGG) enrichment analyses were performed for DEG using clusterProfiler (v3.10.1).

Quantitative real-time PCR (qRT-PCR) analysis

Primers for qRT-PCR were designed using Primer Premier software (5.0) and were synthesized commercially (TIANYI HUIYUAN, Wuhan, China). RNA was isolated using TRI Reagent Solution (Ambion, TR118), according to the manufacturer's instructions. Reverse transcription was performed using HiScript QRT SuperMix for qPCR (Vazyme, Nanjing, China). The primers of HCT and peroxidase genes were listed in

Table S4. β -actin was used as an internal control. Quantitative real-time PCR was subsequently performed using SYBR[®] Select Master Mix (CFX) on a StepOne-Plus[™] Real-Time System (Applied Biosystems). qPCR was performed using the $\Delta\Delta C_t$ method.

Statistical analysis

Pearson correlation coefficients (PCC) between samples were calculated using the `cor` function in R for both transcriptomic and metabolomic data. MSEA, GO, and KEGG enrichment analyses were performed using hypergeometric tests.

Abbreviations

AAS: Atomic absorption spectroscopy; CAT: Catalase; DAM: Differentially abundant metabolite; DEG: Differentially expressed gene; FPKM: Fragments per kilobase of transcript per million fragments mapped; GA: Gibberellin; GO: Gene ontology; HCT: O-hydroxycinnamoyltransferase; ICP-AES: Plasma atomic emission spectroscopy; KEGG: Kyoto Encyclopedia of Genes and Genome; MS: Mass spectrometry; PAL: Phenylalanine ammonia-lyase; PCA: Principal component analysis; PCC: Pearson correlation coefficients; PPO: Polyphenol oxidase; qRT-PCR: Quantitative real-time PCR; SOD: Superoxide dismutase; TMB: Tetramethylbenzidine; UPLC: Ultra-performance liquid chromatography; VIP: Variable importance in projection.

Supplementary Information

The online version contains supplementary material available at <https://doi.org/10.1186/s12870-022-04005-w>.

Additional file 1.

Additional file 2.

Acknowledgements

We thank Mr. Dajie Zhou (Beijing Genomics Institute, Shenzhen, China) for his help on transcriptome sequencing.

Authors' contributions

S.W., C.L. and L.Q. conceived and designed the study; L.Q., C.G., L.W. and D.T. prepared experimental samples; L.Q., B.L., D.W. and W.Z. performed the experiments; Z.H. and S.H. helped to analyze the data; L.Q. and S.L. drew a picture of the article; S.W., C.L. and L.Q. wrote the manuscript. All authors have read and agreed to the published version of the manuscript.

Funding

This research was funded by the Special Project of Guangxi innovation-driven development (Gui ke AA20302016–3) and National Modern Agricultural Industrial System-Banana Innovation Team of Guangxi (nycytxgxtcd-16-01).

Availability of data and materials

The sequencing data generated in the study are deposited to the NCBI SRA database under Bioproject No. PRJNA855237. The data will be released upon publication, and the link for reviewer is: <https://dataview.ncbi.nlm.nih.gov/object/PRJNA855237?reviewer=ltgjsfsohfd875k887agpklgv>

Declarations

Ethics approval and consent to participate

Not applicable.

Consent for publication

Not applicable.

Competing interests

The authors declare that they have no competing interests.

Author details

¹Biotechnology Research Institute, Guangxi Academy of Agricultural Sciences, Nanning 530007, China. ²Biotechnology Research Institute, Guangxi Academy of Agricultural Sciences/National Local Joint Engineering Research Center for Genetic Improvement and Cultivation Techniques of Banana Varieties/National Tropical Fruit Variety improvement Center Guangxi Banana Branch Center, Nanning 530007, China. ³Institute of Plant Protection, Guangxi Academy of Agricultural Sciences, Nanning 530007, China.

Received: 12 August 2022 Accepted: 14 December 2022

Published online: 28 December 2022

References

- Chen J, Xie J, Duan Y, Hu H, Hu Y, Li W. Genome-wide identification and expression profiling reveal tissue-specific expression and differentially regulated genes involved in gibberellin metabolism between Williams banana and its dwarf mutant. *BMC Plant Biol.* 2016;16(1):123.
- Peng J, Richards DE, Hartley NM, Murphy GP, Devos KM, Flintham JE, et al. Green revolution genes encode mutant gibberellin response modulators. *Nature.* 1999;400(6741):256.
- Serrano-Mislata A, Sablowski R. The pillars of land plants: new insights into stem development. *Curr Opin Plant Biol.* 2018;45:11–7.
- Busov VB, Brunner AM, Strauss SH. Genes for control of plant stature and form. *New Phytol.* 2008;177(3):589–607.
- Hedden P, Phillips AL. Gibberellin metabolism: new insights revealed by the genes. *Trends Plant Sci.* 2000;5:523–30.
- Sandoval J, Kerbellec F, Cote F, Doumas P. Distribution of endogenous gibberellins in dwarf and giant off-types banana (*Musa AAA*, cv. grand Nain) plants from in vitro propagation. *Plant Growth Regul.* 1995;17(3):219–24.
- Deng G, Bi F, Liu J, He W, Li C, Dong T, et al. Transcriptome and metabolome profiling provide insights into molecular mechanism of pseudostem elongation in banana. *BMC Plant Biol.* 2021;21(1):125.
- Nemhauser JL, Hong FX, Chory J. Different plant hormones regulate similar processes through largely nonoverlapping transcriptional responses. *Cell.* 2006;126(3):467–75.
- Bidadi H, Yamaguchi S, Asahina M, Satoh S. Effects of shoot-applied gibberellin/gibberellin-biosynthesis inhibitors on root growth and expression of gibberellin biosynthesis genes in *Arabidopsis thaliana*. *Plant Root.* 2010;4:4–11.
- Yamaguchi S, Kamiya Y. Gibberellin biosynthesis: its regulation by endogenous and environmental signals. *Plant Cell Physiol.* 2000;41:251–7.
- Wei YZ, Dong C, Zhang HN, Zheng XW, Shu B, Shi SY, et al. Transcriptional changes in litchi (*Litchi chinensis* Sonn.) inflorescences treated with uniconazole. *PLoS One.* 2017;12(4):e0176053.
- Ahmad I, Kamran M, Ali S, Cai T, Bilegjalgal B, Liu T, et al. Seed filling in maize and hormones crosstalk regulated by exogenous application of uniconazole in semiarid regions. *Environ Sci Pollut Res Int.* 2018;25(33):3225–39.
- Hedden P. The current status of research on gibberellin biosynthesis. *Plant Cell Physiol.* 2020;61(11):1832–49.
- Hernández-García J, Briones-Moreno A, Blázquez MA. Origin and evolution of gibberellin signaling and metabolism in plants. *Semin Cell Dev Biol.* 2021;109:46–54.
- Han F, Zhu B. Evolutionary analysis of three gibberellin oxidase genes in rice, *Arabidopsis*, and soybean. *Gene.* 2011;473(1):23–35.
- Mitchum MG, Yamaguchi S, Hanada A, Kuwahara A, Yoshioka Y, Kato T, et al. Distinct and overlapping roles of two gibberellin 3-oxidases in *Arabidopsis* development. *Plant J.* 2006;45:804–18.
- Huang SS, Raman AS, Ream JE, Fujiwara H, Cerny RE, Brown SM. Overexpression of 20-oxidase confers a gibberellin overproduction phenotype in *Arabidopsis*. *Plant Physiol.* 1998;118:773–81.
- Oikawa T, Koshioka M, Kojima K, Yoshida H, Kawata M. A role of OsGA20ox1, encoding an isoform of gibberellin 20-oxidase, for regulation of plant stature in rice. *Plant Mol Biol.* 2004;55:687–700.

19. Shan C, Mei ZL, Duan JL, Chen HY, Feng HF, Cai WM. OsGA2ox5, a gibberellin metabolism enzyme, is involved in plant growth, the root gravity response and salt stress. *PLoS One*. 2014;9:e87110.
20. Spielmeyer W, Ellis MH, Chandler PM. Semidwarf (sd-1), "green revolution" rice, contains a defective gibberellin 20-oxidase gene. *Proc Natl Acad Sci U S A*. 2002;99:9043–8.
21. Thomas SG, Phillips AL, Hedden P. Molecular cloning and functional expression of gibberellin 2-oxidases, multifunctional enzymes involved in gibberellin deactivation. *Proc Natl Acad Sci U S A*. 1999;96:4698–703.
22. Schomburg FM, Bizzell CM, Lee DJ, Zeevaert JA, Amasino RM. Overexpression of a novel class of gibberellin 2-oxidases decreases gibberellin levels and creates dwarf plants. *Plant Cell*. 2003;15:151–63.
23. D'Hont A, Denoeud F, Aury JM, Baurens FC, Carreel F, Garsmeur O, et al. The banana (*Musa acuminata*) genome and the evolution of monocotyledonous plants. *Nature*. 2012;488:213–7.
24. Wang Y, Xiao X, Wang X, Zeng J, Kang H, Fan X, et al. RNA-Seq and iTRAQ reveal the dwarfing mechanism of dwarf polish wheat (*Triticum polonicum* L.). *Int J Biol Sci*. 2016;12(6):653–66.
25. Pearce S, Saville R, Vaughan SP, Chandler PM, Wilhelm EP, Sparks CA, et al. Molecular characterization of Rht-1 dwarfing genes in hexaploid wheat. *Plant Physiol*. 2011;157:1820–31.
26. Zhang Y, Liu J, Yu J, Zhang H, Yang Z. Relationship between the Phenylpropanoid pathway and dwarfism of *Paspalum seashore* based on RNA-Seq and iTRAQ. *Int J Mol Sci*. 2021;22(17):9568.
27. Foster TM, McAtee PA, Waite CN, Bolding HL, McGhie TK. Apple dwarfing rootstocks exhibit an imbalance in carbohydrate allocation and reduced cell growth and metabolism. *Hortic Res*. 2017;4:17009.
28. Ren Z, Fang M, Muhae-Ud-Din G, Gao H, Yang Y, Liu T, et al. Metabolomics analysis of grains of wheat infected and noninfected with *Tilletia controversa* Kühn. *Sci Rep*. 2021;11(1):18876.
29. Corcoran MR, Geissman TA, Phinney BO. Tannins as gibberellin antagonists. *Plant Physiol*. 1972;49(3):323–30.
30. Green FB, Corcoran MR. Inhibitory action of five tannins on growth induced by several gibberellins. *Plant Physiol*. 1975;56(6):801–6.
31. Izumi K, Iwai T, Oshio H. Growth retarding effects of Uniconazole on plants. *Chemical Regulation of Plants (In Japanese)*. 1989;24:142–6.
32. Dixon RA, Paiva NL. Stress-induced phenylpropanoid metabolism. *Plant Cell*. 1995;7:1085–97.
33. MacDonald MJ, D' Cunha GB. A modern view of phenylalanine ammonia lyase. *Biochem Cell Biol*. 2007;85:273–82.
34. Song J, Wang Z. RNAi-mediated suppression of the phenylalanine ammonia-lyase gene in *Salvia miltiorrhiza* causes abnormal phenotypes and a reduction in rosmarinic acid biosynthesis. *J Plant Res*. 2011;124:183–92.
35. Vanholme R, De Meester B, Ralph J, Boerjan W. Lignin biosynthesis and its integration into metabolism. *Curr Opin Biotechnol*. 2019;56:230–9.
36. Tanaka H, Masuta C, Uehara K, Kataoka J, Koiwai A, Noma M. Morphological changes and hypomethylation of DNA in transgenic tobacco expressing antisense RNA of the S-adenosyl-L-homocysteine hydrolase gene. *Plant Mol Biol*. 1997;35:981–6.
37. Vanholme R, Demedts B, Morreel K, Ralph J, Boerjan W. Lignin biosynthesis and structure. *Plant Physiol*. 2010;153:895–905.
38. Bonawitz N, Chapple C. The genetics of lignin biosynthesis: connecting genotype to phenotype. *Annu Rev Genet*. 2010;44:337–63.
39. Liu Q, Luo L, Zheng L. Lignins: biosynthesis and biological functions in plants. *Int J Mol Sci*. 2018;19(2):335.
40. Maruyama R, Mayuzumi Y, Morisawa J, Kawai S. Transgenic rice plants expressing the α -L-arabinofuranosidase of *Coprinopsis cinerea* exhibit strong dwarfism and markedly enhanced tillering. *Plant Biotechnol (Tokyo)*. 2021;38(3):379–86.
41. Hu WJ, Harding SA, Lung J, Popko JL, Ralph J, Stokke DD, et al. Repression of lignin biosynthesis promotes cellulose accumulation and growth in transgenic trees. *Nat Biotechnol*. 1999;17(8):808–12.
42. Negi S, Tak H, Ganapathi TR. Cloning and functional characterization of MusaVND1 using transgenic banana plants. *Transgenic Res*. 2015;24(3):571–85.
43. Negi S, Tak H, Ganapathi TR. Functional characterization of secondary wall deposition regulating transcription factors MusaVND2 and MusaVND3 in transgenic banana plants. *Protoplasma*. 2016;253(2):431–46.
44. Negi S, Tak H, Ganapathi TR. Overexpression of MusaNAC68 reduces secondary wall thickness of xylem tissue in banana. *Plant Biotechnol rep*. 2019;13:151–60.
45. Liang W, Ni L, Carballar-Lejarazú R, Zou X, Sun W, Wu L, et al. Comparative transcriptome among *Euscaphis konishii* Hayata tissues and analysis of genes involved in flavonoid biosynthesis and accumulation. *BMC Genomics*. 2019;20(1):24.
46. Qu G, Peng D, Yu Z, Chen X, Cheng X, Yang Y, et al. Advances in the role of auxin for transcriptional regulation of lignin biosynthesis. *Funct Plant Biol*. 2021;48(8):743–54.

Publisher's Note

Springer Nature remains neutral with regard to jurisdictional claims in published maps and institutional affiliations.

Ready to submit your research? Choose BMC and benefit from:

- fast, convenient online submission
- thorough peer review by experienced researchers in your field
- rapid publication on acceptance
- support for research data, including large and complex data types
- gold Open Access which fosters wider collaboration and increased citations
- maximum visibility for your research: over 100M website views per year

At BMC, research is always in progress.

Learn more biomedcentral.com/submissions

